

Kinematic analysis and feedrate optimization in six-axis NC abrasive belt grinding of blades

Junteng Wang · Dinghua Zhang · Baohai Wu ·
Ming Luo · Ying Zhang

Received: 21 September 2014 / Accepted: 18 January 2015 / Published online: 7 February 2015
© Springer-Verlag London 2015

Abstract The purpose of this paper is to propose a kinematic analysis and optimization method for a kind of six-axis numerical control (NC) belt grinding machine tools when grinding blades. Six-axis NC abrasive belt grinding machine tools have been widely used for grinding blades in the aero engine manufacturing enterprises. Kinematic analysis and feedrate optimization play an important role in efficient machining with NC machine tools. After analyzing the basic kinematic relation of the six-axis NC abrasive belt grinding machine tool, coordinate systems are established to calculate the generalized kinematics model. The formulas of the rotary angles and the motion coordinates are provided by simultaneously transforming the three vectors which control the motions of the abrasive belt contact disk. An efficient strategy for feedrate optimization is developed to meet the accuracy requirements of blade abrasive belt grinding process. Both the load capacity of process system and the servo drive capability of machine tools are considered. The validity is demonstrated with simulations and experiments on a TX6-1000HV computer numerical control (CNC) machine tool.

Keywords Six-axis · Abrasive belt grinding · Kinematic analysis · Feedrate optimization

1 Introduction

Blades are the most critical components of an aero engine and assembled along the engine stages in different sizes and roles.

J. Wang · D. Zhang (✉) · B. Wu · M. Luo · Y. Zhang
Key Laboratory of Contemporary Design and Integrated
Manufacturing Technology of Ministry of Education, Northwestern
Polytechnical University, Xi'an 710072, China
e-mail: dhzhang@nwpu.edu.cn

A small change in blade geometry can lead to a large change in engine performance. Therefore, it is crucial to guarantee the machining quality of blades and to maintain the blade shape design. Currently, blades are always rough machined by milling. After milling, it is necessary to grind the blade surface because of its high machining precision requirements. A robot belt grinding system has a good prospect for releasing hand grinders from their dirty and noisy work environment [1]. Also, it can greatly improve the machining precision and work efficiency. Therefore, numerical control (NC) belt grinding has been widely used in blade grinding field, and more recently, six-axis computer numerical control (CNC) abrasive belt grinding machine tools have been introduced into the aero engine manufacturing enterprises.

Kinematic analysis is of great importance for the usage of NC machine tools. It plays an important role in the NC postprocessing program development process. Also, it is the basement of feedrate optimization which considers the kinematic characteristics of machine tools. Practically, CAM software generate tool paths considering only the relative position between workpiece and cutter. The tool path data files generated by CAM software always need to be converted into NC files by a specially used postprocessing program which takes the structure characteristics of machine tools into account. The key technology of NC postprocessing is the kinematic analysis of machine tools.

Generally speaking, machining with six-axis machine tools can obtain higher machining precision and working efficiency. However, as six-axis machine tools have six degrees of freedom, it makes the control method of grind wheel be greatly complex, which may have a bad effect on the machining precision. Moreover, the machine's capability is an important issue affecting the efficiency of the CNC interpolator. The maximum feedrate, acceleration/deceleration, and jerk that can be output by a servo motor are generally limited and should be specified in the design of the kinematic profiles

[2]. The velocity or the acceleration may exceed their limits even if the feedrate remains a small value. If the exceeding conditions happen, the motion of machine tools would be unsteady because of servo delays. It may lead to increases in error, surface quality questions, cutting tool wear, and other bad issues. This problem is closely related with the machine structure, which makes it hard to solve when programming with CAM software. Kinematic analysis of machine tools gives it a chance to solve this problem with feedrate optimization.

Kinematic analysis of a machine tool is intended to make clear the relationships among moving elements and obtain the motion coordinate of each axis when machining, which makes it be the basic and key technology of the postprocessing for machine tools. It can be accomplished through a series of transformation among the coordinate systems set up on the machine elements, which are similar to arms of robot. Many scientists have done great works in this field. Sakamoto and Inasaki [3] classified the configuration of commercial five-axis machine tools into three types. Based on this, Lee and She [4, 5] described the three types of five-axis machine tools by a generalized kinematic structure and presented the method for deriving the complete analytical NC code expressions. More practically, Bohez [6] investigated the geometric and kinematic properties of five-axis machine tools such as workspace utilization factor and machine tool space efficiency by modeling the machine tool kinematics. In the same year, Jung et al. [7] analyzed the kinematic properties for a typical five-axis milling machine of table-rotating/tilting type and proposed two efficient algorithms for the postprocessing considering the characteristics of TRT-type machines. Later, Tutunea-Fatan and Feng [8] presented a generic and unified model for all the five-axis machine tools with two rotational axes, analyzed the kinematic characteristics, and derived a general coordinate transformation matrix for five-axis machine tools. Similarly, Sørby [9] examined the inverse kinematics of a five-axis machine tool and proposed an approach for avoiding kinematic singularities. She and Chang [10] later extended their previous researches and developed a generic five-axis postprocessor system from a generalized kinematics model adding four rotational degrees of freedom where two of them are applied to the workpiece table and the other two are applied to the spindle. Also, they accomplished a kinematic analysis of the machine tools and gave the complete analytical solutions of NC data dealing with different configurations effectively. Recently, Boz and Lazoglu [11] introduced a postprocessor for table-tilting-type five-axis machine tool based on generalized kinematics with variable feedrate implementations. Furthermore, they presented a method for avoiding kinematic singularities by spherical interpolation and NC data correction is presented as well.

Based on the kinematic analysis, feedrate can be optimized, and the objective is to obtain a more suitable feedrate profile which makes best use of the kinematical characteristics of

machine tools while the machining quality is assured. Various studies have addressed this issue. The identification of an optimal feed profile without exceeding the saturation limits of the actuators was first studied mainly by the robotics researchers. Bobrow et al. [12] and Shin and McKay [13] were the first to solve the minimum time control problem. They proved that the actuator torque constraints limit the velocity along the manipulator path. They controlled the acceleration between its maximum and minimum limits at the identified path points to generate a bang-bang style trajectory. In recent years, more researches were focused on the CNC machine tools. Lavernhe et al. [14] proposed a predictive model of kinematical performance in five-axis milling within the context of high-speed machining. The capacities of each axis as well as NC unit functions can be expressed as limiting constraints for feedrate prediction. Sencer et al. [15] presented a feed scheduling algorithm for CNC systems to minimize the machining time for five-axis contour machining of sculptured surfaces. The velocity, acceleration, and jerk limits of the five axes were considered in finding the most optimal feed along the tool path in order to ensure smooth and linear operation of the servo drives with minimal tracking error. Beudaert, Pechard, Tournier [16] smoothed 5-axis tool paths based on drive constraints in order to maximize the real feedrate and to reduce the machining time. Based on their previous works, Beudaert et al. [17] later controlled each axis kinematical parameter based on a decoupled approach which separates the problem of geometrical treatment of the programmed tool path and of feedrate interpolation. Recently, Erkorkmaz et al. [18] presented a novel and comprehensive strategy for planning minimum cycle time tool trajectories, subject to both machining process and machine tool drive limits. They computed the workpiece-tool engagement along the tool path and set local feed limits to maintain a specified resultant cutting force. Also, they limited the velocity, acceleration, and jerk magnitudes commanded to each actuator.

Most of these studies focused on five-axis NC milling machine tools, and the researchers accomplished a kinematic analysis and optimization for almost all types of five-axis NC milling machine tools in these studies. However, few studies have paid attention to the kinematics of six-axis CNC abrasive belt grinding machine tools which have a more complex motion control mechanism when grinding blades; in this situation, six freedoms are considered and three control vectors are introduced. What's more, the surface cutting feedrate which has an effect on the grinding quality was not taken into account in past literatures.

The goal of this paper is to propose a kinematic analysis and optimization method for six-axis NC belt grinding machine tools when grinding blades. The paper is organized as follows. Section 2 deals with the kinematic analysis of the machine tools. The formulas of the rotary angles and the motion coordinates are calculated in this part. Section 3 is

dedicated to the feedrate optimization. A feedrate optimization is made considering both the load capacity of process system and the servo drive capability of machine tools. Section 4 validates the method through a machining example. Experiment and simulation are also carried out in this part. At last, this paper ends with some conclusions.

2 Kinematic analysis

2.1 Machine tool structure and code format

A kind of six-axis NC belt grinding machine tools used for grinding and polishing the surface of aero engine blades is focused on in this paper. The structure is shown in Fig. 1. This type of machine tools has moving spindles in X , Y , and Z -direction and rotating tables with respect to A -, B -, and C -axis. The belt mechanism which moves along the X , Y -direction with the column adapts horizontal arrangement. When machining, the blade is fixed on the A -axis rotary table. The directions marked in Fig. 1 are the positive directions of each CNC axis motion.

The format of cutter location points is defined as $(B_x, B_y, B_z, iw, jw, kw, im, jm, km)$, where (B_x, B_y, B_z) is the center coordinate vector of the abrasive belt contact disk, (iw, jw, kw) is the supporting axial vector which is similar with the tool axis vector of milling cutters, and (im, jm, km) is the axial vector of the abrasive belt contact disk. All of the three vectors are defined in the workpiece coordinate system. The center coordinate vector (B_x, B_y, B_z) is used to define the location of abrasive belt contact disk while the other two are used to control the attitude of the abrasive belt contact disk. Three vectors are combined to define the motion of the abrasive belt contact disk, as shown in Fig. 2.

2.2 Kinematic transformation

The kinematic analysis of machine tools is attended to make clear the motion transmission of mechanical system and obtain

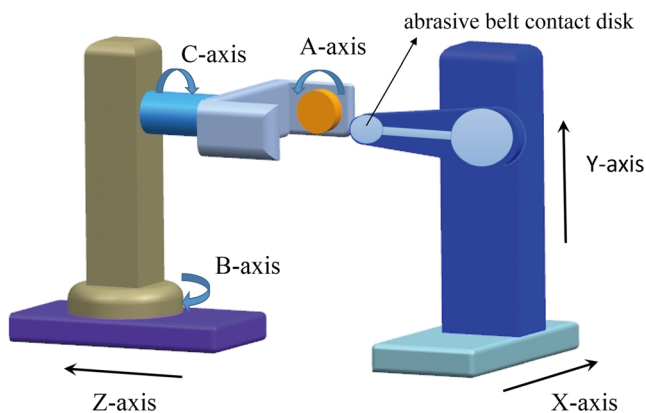


Fig. 1 Structure of the six-axis NC belt grinding machine tools

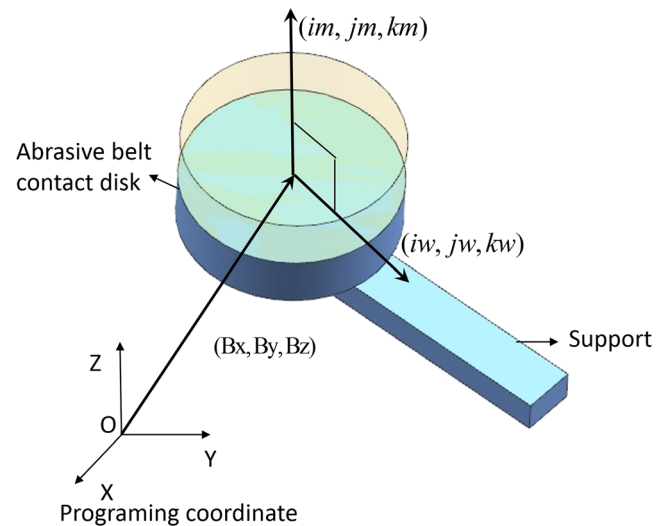


Fig. 2 Control vectors of the abrasive belt contact disk

the machine tools' motion coordinates. For this purpose, the generalized kinematics model needs to be calculated for converting the relative movement between the tool and workpiece into the movement of machine tools' moving parts. The transformation between the workpiece coordinate system and the cutter coordinate system is accomplished through analyzing the series local coordinate systems which are established, respectively, on the tool, workpiece, and other moving elements.

2.2.1 Establishment of coordinate systems

The tool motion of multi-axis CNC machine tools is controlled by a kinematic chain which is made up of moving elements connected in sequence. The kinematic chain consists of translational and rotary joints. The synthetic motion of all the moving elements forms the real cutting motion. By analyzing the machine structure shown in Fig. 1, the kinematic chain can be built up as shown in Fig. 3.

Local coordinate systems, as shown in Fig. 4, are established on the tool, workpiece, and other moving

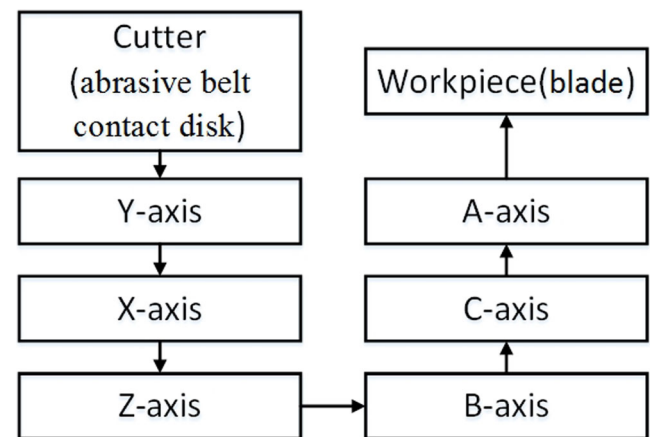
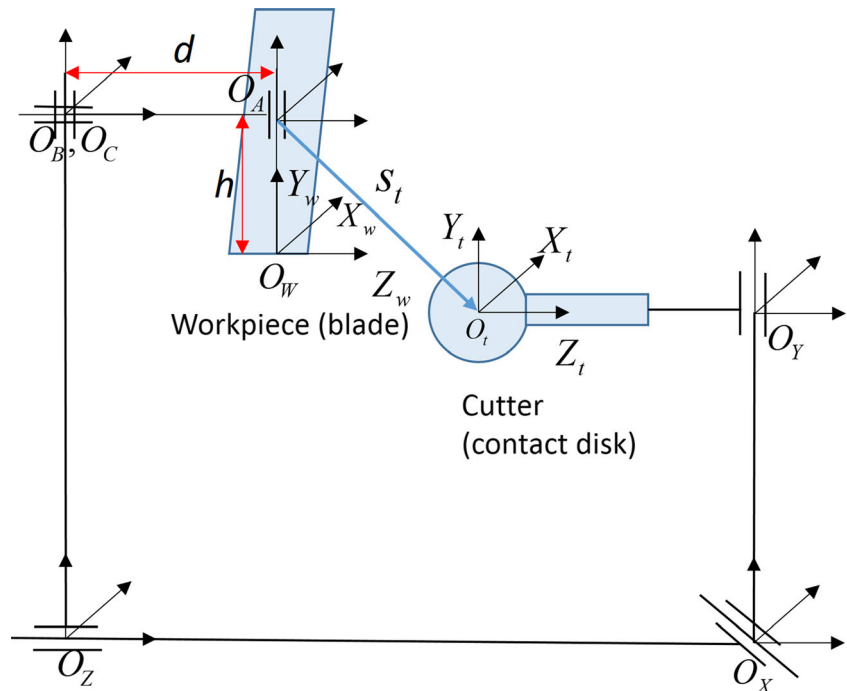


Fig. 3 Kinematic chain of the machine tools

Fig. 4 Coordinate systems for transformation matrix



elements at the initial state to further describe the motion of machine tools, where $O_w X_w Y_w Z_w$ (O_w for short) is the workpiece coordinate system which is set up on the machining blade, and it is also the program coordinate system. $O_t X_t Y_t Z_t$ (O_t for short) is the cutter coordinate system whose origin is set at the cutter location point and initial direction is the same with the world coordinate system. Similarly, the coordinate systems O_A , O_B , O_C , O_X , O_Y and O_Z are established on the other moving elements, respectively. The origin of O_t coincides with the origin of O_A when the machine tool is at the initial state, which means $s_t(X, Y, Z)$ is the location vector of translational joints relative to the initial state. The distance values between contiguous local coordinate systems are shown in Fig. 4.

2.2.2 Calculation of transformation matrices

The local coordinate systems have been established in Sect. 2.2.1; as all the motion pairs are connected in series, the overall transformation matrix of the transformation from coordinate system O_t to O_w can be obtained by multiplying the transformation matrices between contiguous local coordinate systems. In this part, the transformation matrices of translational and revolute pairs will be calculated, respectively, and the overall transformation matrix will be obtained finally.

Assume O_i and O_j are two local coordinate systems which are established on two arbitrarily contiguous moving elements i and j . The moving elements i and j are connected by a

kinematic pair. Let Q_{ji} be the transformation matrix of the transformation from O_i to O_j .

If the connecting kinematic pair is a prismatic pair, then

$$Q_{ji} = P(r_{ji}) \cdot T(s_{ji}) \tag{1}$$

Where $P(r_{ji})$ is a translation transformation matrix defined by the initial positional relationship between the two local coordinate systems, $r_{ji}(x_{ji}, y_{ji}, z_{ji})$ is the position vector of the origin of coordinate O_i in O_j , and

$$P(r_{ji}) = \begin{bmatrix} 1 & 0 & 0 & x_{ji} \\ 0 & 1 & 0 & y_{ji} \\ 0 & 0 & 1 & z_{ji} \\ 0 & 0 & 0 & 1 \end{bmatrix} \tag{2}$$

Where $T(s_{ji})$ is a translation transformation matrix; assume $s_{ji}(sx_{ji}, sy_{ji}, sz_{ji})$ is the translation vector, then

$$T(s_{ji}) = \begin{bmatrix} 1 & 0 & 0 & sx_{ji} \\ 0 & 1 & 0 & sy_{ji} \\ 0 & 0 & 1 & sz_{ji} \\ 0 & 0 & 0 & 1 \end{bmatrix} \tag{3}$$

If the kinematic pair is a revolute pair, then

$$Q_{ji} = P(r_{ji}) \cdot R(\theta_{ji}) \tag{4}$$

Where $R(\theta_{ji})$ is a rotation transformation matrix and θ_{ji} is the counterclockwise rotation angle of the revolute pair. Assume the values of the counterclockwise rotation angles along with X -, Y -, and Z -axis are A , B , and C , respectively, then

if the revolute pair rotates along with X -axis,

$$R(\theta_{ji}) = R(A) = \begin{bmatrix} 1 & 0 & 0 & 0 \\ 0 & \cos A & -\sin A & 0 \\ 0 & \sin A & \cos A & 0 \\ 0 & 0 & 0 & 1 \end{bmatrix} \tag{5}$$

If the revolute pair rotates along with Y -axis,

$$R(\theta_{ji}) = R(B) = \begin{bmatrix} \cos B & 0 & \sin B & 0 \\ 0 & 1 & 0 & 0 \\ -\sin B & 0 & \cos B & 0 \\ 0 & 0 & 0 & 1 \end{bmatrix} \tag{6}$$

If the revolute pair rotates along with Z -axis,

$$R(\theta_{ji}) = R(C) = \begin{bmatrix} \cos C & -\sin C & 0 & 0 \\ \sin C & \cos C & 0 & 0 \\ 0 & 0 & 1 & 0 \\ 0 & 0 & 0 & 1 \end{bmatrix} \tag{7}$$

Based on this, the transformation matrices between local coordinate systems can easily be obtained by analyzing the motion relation of kinematic pairs.

Finally, the overall transformation matrix Q_{wt} can be derived by multiplication of the transformation matrices between each two contiguous local coordinate systems based on the basic motion relation of machine tool:

$$Q_{wt} = Q_{wn} \cdot Q_{n-1} \cdot Q_{n-1-n-2} \cdot \dots \cdot Q_{32} \cdot Q_{21} \cdot Q_{1t} \tag{8}$$

For the machine tool shown in Fig. 1, the cutter coordinate system is established on the center of the abrasive belt contact disk, and the overall transformation matrix is derived as the following:

$$Q_{wt} = Q_{wA} \cdot Q_{AC} \cdot Q_{CB} \cdot Q_{BZ} \cdot Q_{ZX} \cdot Q_{XY} \cdot Q_{Yt} = \begin{bmatrix} 1 & 0 & 0 & h \\ 0 & 1 & 0 & 0 \\ 0 & 0 & 1 & 0 \\ 0 & 0 & 0 & 1 \end{bmatrix} \cdot \begin{bmatrix} 1 & 0 & 0 & 0 \\ 0 & \cos A & -\sin A & 0 \\ 0 & \sin A & \cos A & 0 \\ 0 & 0 & 0 & 1 \end{bmatrix} \cdot \begin{bmatrix} 1 & 0 & 0 & 0 \\ 0 & 1 & 0 & 0 \\ 0 & 0 & 1 & -d \\ 0 & 0 & 0 & 1 \end{bmatrix} \cdot \begin{bmatrix} \cos C & -\sin C & 0 & 0 \\ \sin C & \cos C & 0 & 0 \\ 0 & 0 & 1 & 0 \\ 0 & 0 & 0 & 1 \end{bmatrix} \cdot \begin{bmatrix} \cos B & 0 & \sin B & 0 \\ 0 & 1 & 0 & 0 \\ -\sin B & 0 & \cos B & 0 \\ 0 & 0 & 0 & 1 \end{bmatrix} \cdot \begin{bmatrix} 1 & 0 & 0 & X \\ 0 & 1 & 0 & Y \\ 0 & 0 & 1 & Z+d \\ 0 & 0 & 0 & 1 \end{bmatrix} \tag{9}$$

Where the parameters h and d have been given in Fig. 4, d is determined by the machine structure and h can be measured during a machining process.

2.2.3 Solution for motion coordinates

It can be seen from the format of cutter location points that three vectors define the position and attitude of abrasive belt

contact disk simultaneously. Correspondingly, all the three vectors must be transformed to ensure the synthetic motion of moving elements accord with the tool path. In addition, the three vectors transforming procedure simplifies the solving processes of transformation equations, and the motion coordinates of machine tools can be derived easily.

The generalized kinematics model is proposed by transforming these three vectors.

Transformation of the supporting axial vector of abrasive belt contact disk is as follows:

$$[iw, jw, kw, 0]^T = Q_{wt} \cdot [0, 0, 1, 0]^T \tag{10}$$

Transformation of the axial vector of abrasive belt contact disk is as follows:

$$[im, jm, km, 0]^T = Q_{wt} \cdot [1, 0, 0, 0]^T \tag{11}$$

Transformation of the center coordinate vector of abrasive belt contact disk is as follows:

$$[Bx, By, Bz, 1]^T = Q_{wt} \cdot [0, 0, 0, 1]^T \tag{12}$$

By substituting Q_{wt} derived from Eq. (9) into Eqs. (10), (11), and (12), three systems of equations can be obtained as following:

$$\begin{cases} iw = \sin B \cos C \\ jw = \cos A \sin B \sin C - \sin A \cos B \\ kw = \sin A \sin B \sin C + \cos A \cos B \end{cases} \tag{13}$$

$$\begin{cases} im = \cos B \cos C \\ jm = \cos A \cos B \sin C + \sin A \sin B \\ km = \sin A \cos B \sin C - \cos A \sin B \end{cases} \tag{14}$$

$$\begin{cases} Bx = \cos B \cos C \cdot X - \sin C \cdot Y + \sin B \cos C \cdot Z + \sin B \cos C \cdot d + h \\ By = (\cos A \cos B \sin C + \sin A \sin B) \cdot X + \cos A \cos C \cdot Y + (\cos A \sin B \sin C - \sin A \cos B) \cdot Z + (\cos A \sin B \sin C - \sin A \cos B + \sin A) \cdot d \\ Bz = (\sin A \cos B \sin C - \cos A \sin B) \cdot X + \sin A \cos C \cdot Y + (\sin A \sin B \sin C + \cos A \cos B) \cdot Z + (\sin A \sin B \sin C + \cos A \cos B - \cos A) \cdot d \end{cases} \tag{15}$$

By combining and solving Eqs. (13) and (14) on the basis of the actual motion relation of the machine tool, the motion coordinates of the machine tool can be determined as the following:

$$B = \begin{cases} \arctan \left| \frac{iw}{im} \right| & \frac{iw}{im} >= 0 \\ -\arctan \left| \frac{iw}{im} \right| & \frac{iw}{im} < 0 \\ \frac{\pi}{2} \text{ or } -\frac{\pi}{2} & im = 0 \end{cases} \tag{16}$$

For the case when $im=0$, the value of rotation angle B reaches its limit value, which happens very few in actual processing. As workpiece is on the operator side when $B = \frac{\pi}{2}$, let $B = \frac{\pi}{2}$ here in order to monitor the machining situation conveniently.

$$C = \begin{cases} \arccos\left|\frac{im}{\cos(B)}\right| & im > 0 \quad jm \geq 0 \\ 2\pi - \arccos\left|\frac{im}{\cos(B)}\right| & im > 0 \quad jm < 0 \\ \pi - \arccos\left|\frac{im}{\cos(B)}\right| & im < 0 \quad jm \geq 0 \\ \pi + \arccos\left|\frac{im}{\cos(B)}\right| & im < 0 \quad jm < 0 \\ -\arccos(iw) & im = 0 \quad jm < 0 \\ \arccos(iw) & im = 0 \quad jm \geq 0 \end{cases} \quad (17)$$

$$\begin{cases} \sin A = \frac{\sin B \cdot \sin C \cdot kw - \cos B \cdot jw}{\sin B^2 \cdot \sin C^2 + \cos B^2} \\ \cos A = \frac{\cos B \cdot kw + \sin B \cdot \sin C \cdot jw}{\sin B^2 \cdot \sin C^2 + \cos B^2} \end{cases} \quad (18)$$

$$A = \begin{cases} \arcsin(|\sin A|) & \sin A \geq 0 \quad \cos A \geq 0 \\ \pi - \arcsin(|\sin A|) & \sin A \geq 0 \quad \cos A < 0 \\ \pi + \arcsin(|\sin A|) & \sin A < 0 \quad \cos A \geq 0 \\ 2\pi - \arcsin(|\sin A|) & \sin A < 0 \quad \cos A < 0 \end{cases} \quad (19)$$

By substituting the values of A , B , and C into Eq. (15), the values of translational coordinates X , Y , and Z can be derived finally.

3 Feedrate optimization

Feedrate has an important influence on the efficiency, accuracy, and surface quality of machining. A constant contact force throughout the grinding process is necessary to provide a smooth finish on the workpiece [19]. A constant feedrate is often taken when programming for blade grinding to obtain a constant contact force. Feedrate is kept constant in order to maintain cutting condition at a steady state, which means the feedrate refers to a constant surface cutting feedrate. Furthermore, the running precision of each axis must be assured to keep machine tool running steadily. Nowadays, machine tools have possessed certain abilities of motion monitoring and modification for alerting operators and realizing automated processing when the motion parameters exceed their limit values. However, it reduces the processing efficiency and is limited by the processing speed. Thus, feedrate optimization considering kinematic analysis of machine tools before machining can effectively improve the smoothness of machine

tools' motion, and it is important for high efficient machining realization.

3.1 Feedrate optimization based on the extended linear displacement method

The feedrate instructions in tool path files refer to the servo control velocity of each moving axis. Actually, only a unified value is given instead of a value for each moving axis, respectively. The servo control velocities of each moving axis are determined by their motion quantity. The actual surface cutting feedrate with a same feedrate can be different because the linear and rotary motions differ in different program segments. Feedrate can be treated as actual surface cutting feedrate if only linear motion exists. Thus, the feedrate needs to be modified to realize the machining process with a same cutting feedrate when grinding blades. It is well known that NC system controls the linear motion and rotary motion in the same way based on the extended linear displacement method which treats 1° as the same with 1 mm. Next, the feedrate will be modified base on this fact.

Assume (p_{w0}, u_{w0}, v_{w0}) and (p_{w1}, u_{w1}, v_{w1}) are two adjacent cutter locations, $\Delta X, \Delta Y, \Delta Z, \Delta A, \Delta B$, and ΔC are the motion values of each axis between the two adjacent cutter locations. Based on the extended linear displacement method, the motion equivalent ΔS can be calculated as the following:

$$\Delta S = \sqrt{(\Delta X)^2 + (\Delta Y)^2 + (\Delta Z)^2 + (\Delta A)^2 + (\Delta B)^2 + (\Delta C)^2} \quad (20)$$

The feedrate F given in the tool path files refers to the equivalent displacement of cutter per time unit. The execution time T of this program segment is calculated as:

$$T = \frac{\Delta S}{F} \quad (21)$$

Then, the actual cutting feedrate f of abrasive belt contact disk can be calculated as:

$$f = \frac{\delta S}{T} = F \cdot \frac{\delta S}{\Delta S} \quad (22)$$

Where $\delta S = |p_{w1} - p_{w0}|$ is the distance between the two adjacent cutter locations in the workpiece coordinate system which is actual motion displacement of the abrasive belt contact disk.

Finally, the feedrate F can be modified according to the actual surface cutting feedrate f given in the processing technology as following:

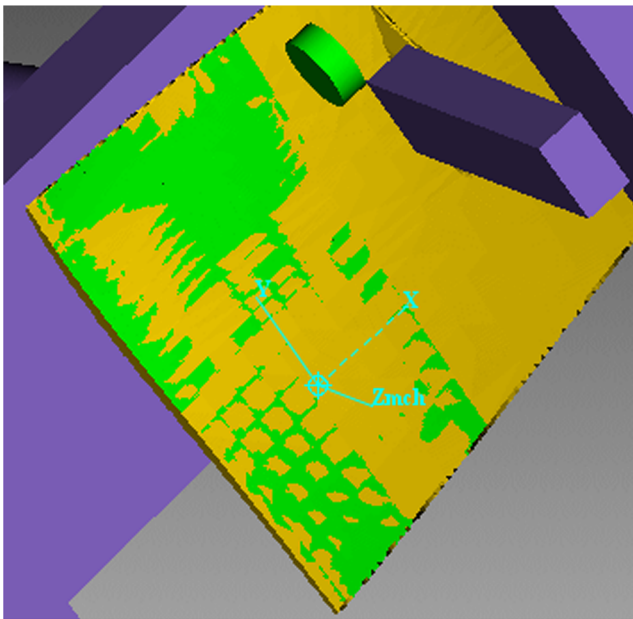


Fig. 5 Simulation result with VERICUT

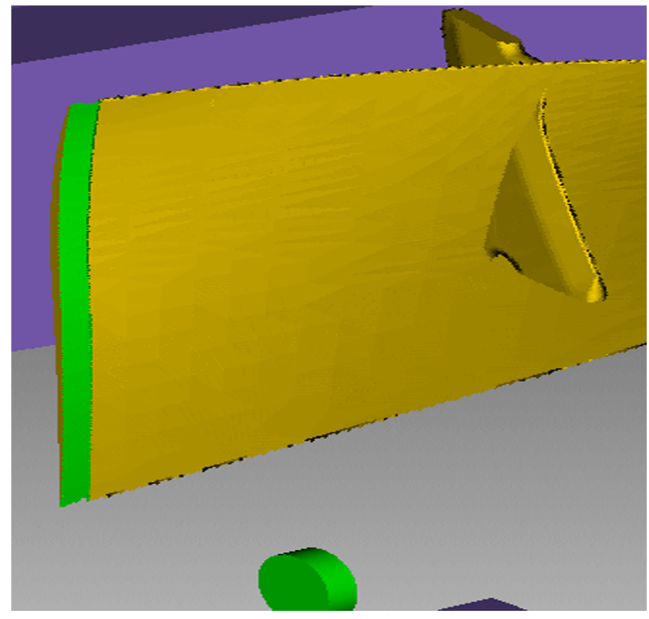


Fig. 6 The cutting row (green row on the blade) for the practical example

$$F = f \cdot \frac{\Delta S}{\delta S} = f \cdot \frac{\sqrt{(\Delta X)^2 + (\Delta Y)^2 + (\Delta Z)^2 + (\Delta A)^2 + (\Delta B)^2 + (\Delta C)^2}}{|p_{w1} - p_{w0}|} \quad (23)$$

3.2 Feedrate optimization considering drive constraints

The feedrate F has been optimized preliminarily considering the load capacity of machining system in Sect. 3.1 in order to obtain a constant cutting feedrate. However, sometimes, the constant value of the cutting feedrate f is set unsuitable, which makes the optimized feedrate reach a large value and the motion parameters exceed their limits. It may cause bad damages to the machining quality and even the running precision of machine tools. This problem must be dealt with even when the cutting feedrate cannot keep constant. Thus, further optimization of feedrate is done with the servo drive capability of machine tools taken into account by building a motion constraints model according to the kinematic analysis of machine tools.

The machine tool drive constraints are the velocity, acceleration, and jerk limits of all active linear and rotary feed

Table 1 Velocity limits of six drives

| | Drives | | | | | |
|-----------------|----------|----------|----------|--------|----------|----------|
| | X-axis | Y-axis | Z-axis | A-axis | B-axis | C-axis |
| Velocity limits | 24 m/min | 24 m/min | 24 m/min | 46 rpm | 33.7 rpm | 33.7 rpm |

drives. It is possible to express the velocity of the drives \dot{q} as a function of the geometry q_s multiplied by a function of the motion using the formula for the derivative of the composition of two functions (Eq. (24)). The acceleration \ddot{q} and jerk \dddot{q} of the drives can be obtained identically in Eqs. (25–26):

$$\dot{q} = \frac{dq}{dt} = \frac{dq}{ds} \frac{ds}{dt} = q_s \dot{s} \quad (24)$$

$$\ddot{q} = q_{ss} \dot{s}^2 + q_s \ddot{s} \quad (25)$$

$$\dddot{q} = q_{sss} \dot{s}^3 + 3q_{ss} \dot{s} \ddot{s} + q_s \dddot{s} \quad (26)$$

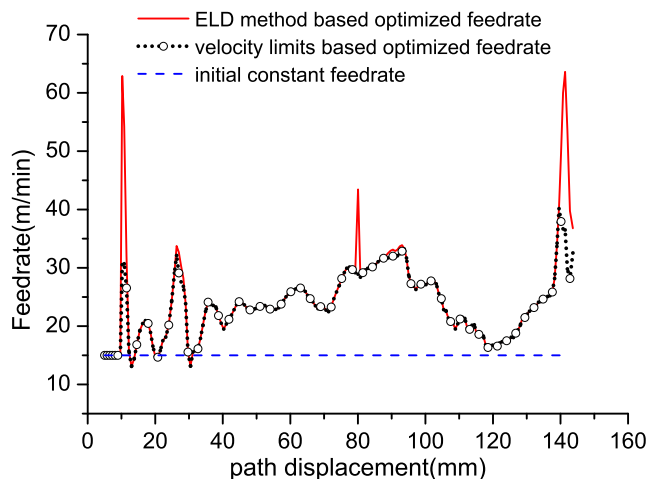


Fig. 7 Optimized and initial feed profiles

Where s is the path displacement along the tool path, $q=q(s)=[X(s),Y(s),Z(s),A(s),B(s),C(s)]^T$ are the axis position interpolation vector function and its six scalar components, $\dot{q} = [\dot{X}(s), \dot{Y}(s), \dot{Z}(s), \dot{A}(s), \dot{B}(s), \dot{C}(s)]$ is the axes velocity, $\ddot{q} = [\ddot{X}(s), \ddot{Y}(s), \ddot{Z}(s), \ddot{A}(s), \ddot{B}(s), \ddot{C}(s)]$ is the axes acceleration, $q = [X(s), Y(s), Z(s), A(s), B(s), C(s)]$ is the axes jerk, q_s, q_{ss} , and q_{sss} are derivatives of the axis positions, and \dot{s}, \ddot{s} , and \ddot{s} refer to the tangential velocity (feed), acceleration, and jerk profiles as a function of the path displacement, respectively.

The velocities, accelerations, and jerks of six drives given in Eqs. (24–26) must not exceed their saturation limits. Thus, the following set of equations is obtained, respectively, for the velocity, acceleration, and jerk constraints:

$$|j \dot{q}^i| \leq V_{\max}^i; \quad |j \ddot{q}^i| \leq A_{\max}^i; \quad |j \ddot{q}^i| \leq J_{\max}^i \quad (27)$$

Where $i=X, Y, Z, A, B, C$ represents each axis of the machine tools, $j=1, \dots, N$ is the discretized value along the path, V_{\max}

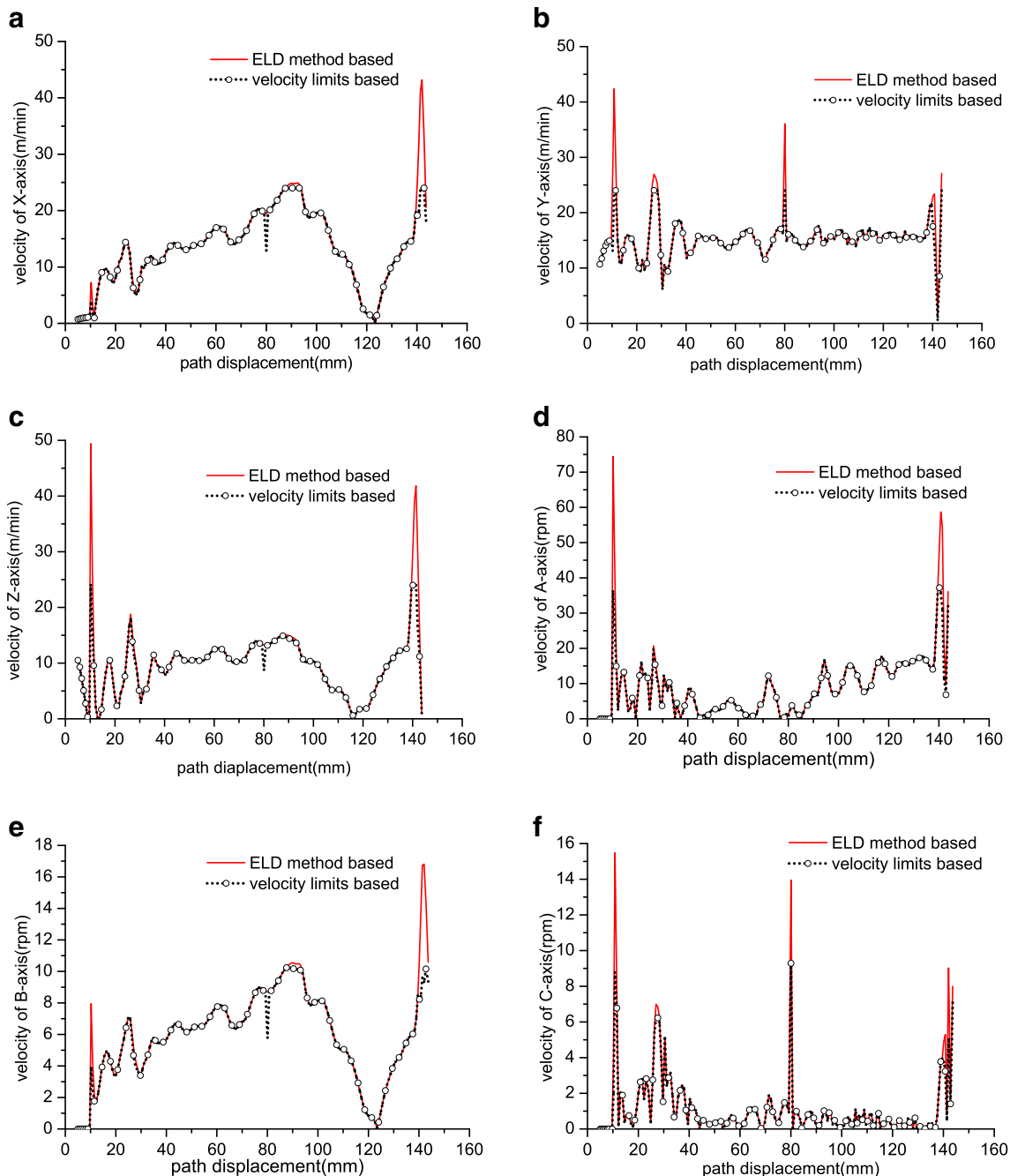


Fig. 8 Comparisons between velocity limits-based optimized and un-optimized velocity profiles (a, b, c, d, e, and f)

$= [V_{\max}^X \ V_{\max}^Y \ V_{\max}^Z \ V_{\max}^A \ V_{\max}^B \ V_{\max}^C]$ is the axes velocity limits, and A_{\max} and J_{\max} are the limits of axes acceleration and jerk identically.

Optimization considering the velocity constraints is discussed in detail here, and the acceleration and jerk constraints can be handled similarly. As we know, the velocity of each axis must be within limits, which means a modification should be taken for each machine axis velocities by the same proportion when some motion axis velocities exceed their fair values. Take X -axis for example, if its velocity exceeds the limits, then the feedrate should be modified as the following:

$$F = V_{\max}^X \cdot \frac{\Delta S_j}{\Delta X_j} \quad (28)$$

4 Simulation and experimental results

The simulation was carried out with VERICUT software. A postprocessor was developed based on the kinematic analysis. The CL data for grinding the blade is generated by the Unigraphics CAM module and then converted to the NC code by the developed postprocessor software. The result is shown in Fig. 5, the abrasive belt contact disk moves along the tool path well, which verifies that the kinematic analysis is feasible and correct.

The feedrate optimization algorithm of this paper was validated by a practical example. In this example, a TX6-1000HV six-axis CNC abrasive belt grinding machine tool was used. Its structure is the same with the structure shown in Fig. 1 and drive velocity constraints are given by its supplier in Table 1. The motion of the abrasive belt contact disk which moves along the cutting row (Fig. 6) was optimized in accordance with our algorithm. The initial feedrate was set to be 15 m/min and optimized by the axes velocity limits after being controlled by the extended linear displacement method. The optimized feedrate is illustrated in Fig. 7. It can be seen in



Fig. 9 TX6-1000HV machine tool for experiment

Fig. 7 that the feedrate controlled by the extended linear displacement method changes rapidly and reaches high values sometimes. It is because that the rotary axes have violent movements when grinding blades, which means the velocities of rotary axes tend more to exceed their fair values. The feedrate optimized by the axes velocity limits reaches a more steady state and the peak values are decreased. The optimized velocities of each axis are compared with the extended linear displacement (ELD)-optimized ones in Fig. 8. As is shown in Fig. 8, the optimized velocities of each axis are successfully limited under their fair values, which validates our algorithm.

Finally, the optimized NC program was tested in actual processing, the experiments were conducted on the TX6-1000HV six-axis CNC abrasive belt grinding machine tool (Fig. 9). A Siemens Sinumerik 840D industrial NC controller is used by the machine tool. The machining result is shown in Fig. 10. It satisfies the demands of enterprises and demonstrates that the proposed methodology can be successfully applied to the practical machining.

5 Conclusion

Six-axis CNC abrasive belt grinding machines have been widely used in the blade processing enterprises, which makes the efficiency and precision of blade machining be largely improved. In its practical applications, the tool path files generated by CAM software need to be converted to NC files, which calls for specially used postprocessing programs. To overcome this issue, this paper presents a kinematic analysis for a class of six-axis NC belt grinding machine tools with similar structures when grinding blades. Also, the formula of the rotary angles and the motion coordinates is provided which can be directly used in the postprocessing.

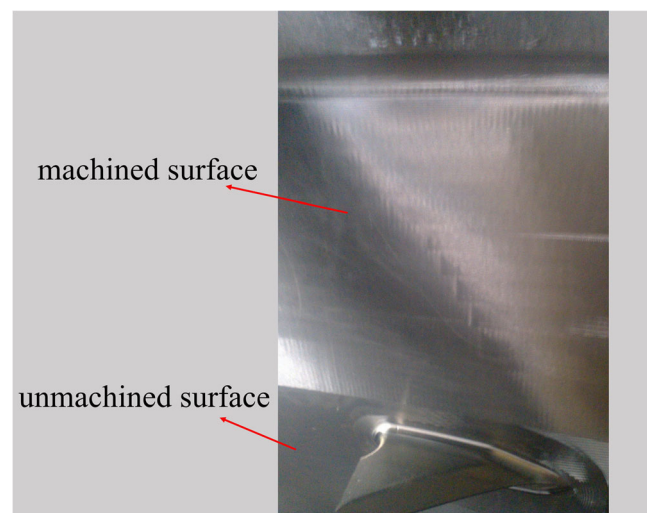


Fig. 10 Experiment result

The kinematic analysis makes it possible to optimize the grinding procedure on the basis of machine structure characteristics. A constant surface cutting feedrate is usually used when grinding blades. In this paper, feedrate is optimized firstly based on the constant cutting feedrate. However, each axis kinematical parameter may exceed their limits if the constant value of the cutting feedrate is set unsuitable, which causes heavy damage to the machining quality and even the running precision of machine tools. To solve this problem, feedrate optimization considering the servo drive capability of machine tools is done in this paper. The results of a practical example showed that the optimization considering machine tool drive constraints can greatly improve the motion of six-axis CNC abrasive belt grinding machine tool when grinding blades.

The research results have been successfully tested on a TX6-1000HV six-axis CNC abrasive belt grinding machine tool. The results can also serve as references to the kinematic analysis and optimization of other types of six-axis CNC machine tools.

References

1. Song YX, Lv HB, Yang ZH (2012) An adaptive modeling method for a robot belt grinding process. *IEEE/ASME Trans Mechatron* 17(2): 309–317
2. Lai JY, Lin KY, Tseng SJ, Ueng WD (2008) On the development of a parametric interpolator with confined chord error, feedrate, acceleration and jerk. *Int J Adv Manuf Technol* 37:104–121
3. Sakamoto S, Inasaki I (1993) Analysis of generating motion for five-axis machining centers. *Trans Jpn Soc Mech Eng C* 59(561):1553–1559 (in Japanese)
4. Lee RS, She CH (1997) Developing a postprocessor for three types of five-axis machine tools. *Int J Adv Manuf Technol* 13(9):658–665
5. She CH, Lee RS (2000) A postprocessor based on the kinematics model for general five-axis machine tools. *J Manuf Process* 2(2): 131–141
6. Bohez ELJ (2002) Five-axis milling machine tool kinematic chain design and analysis. *Int J Mach Tool Manuf* 42(4):505–520
7. Jung YH, Lee DW, Kim JS, Mok HS (2002) NC post-processor for 5-axis milling machine of table-rotating/tilting type. *J Mater Process Technol* 130:641–646
8. Tutunea-Fatan OR, Feng HY (2004) Configuration analysis of five-axis machine tools using a generic kinematic model. *Int J Mach Tool Manuf* 44(11):1235–1243
9. Sørbø K (2007) Inverse kinematics of five-axis machines near singular configurations. *Int J Mach Tool Manuf* 47(2):299–306
10. She CH, Chang CC (2006) Design of a generic five-axis postprocessor based on generalized kinematics model of machine tool. *Int J Mach Tool Manuf* 47(3):537–545
11. Boz Y, Lazoglu I (2013) A postprocessor for table-tilting type five-axis machine tool based on generalized kinematics with variable feedrate implementation. *Int J Adv Manuf Technol* 66(9):1285–1293
12. Bobrow JE, Dubowsky S, Gibson J (1985) Time-optimal control of robotic manipulators along specified paths. *Int J Robot Res* 4(3):3–17
13. Shin K, McKay N (1985) Minimum-time control of robotic manipulators with geometric path constraints. *IEEE Trans Autom Control* 30(6):531–541
14. Sencer B, Altintas Y, Croft E (2008) Feed optimization for five-axis CNC machine tools with drive constraints. *Int J Mach Tool Manuf* 48(7):733–745
15. Lavernhe S, Tournier C, Lartigue C (2008) Kinematical performance prediction in multi-axis machining for process planning optimization. *Int J Adv Manuf Technol* 37(5):534–544
16. Beudaert X, Pechar PY, Tournier C (2011) 5-Axis tool path smoothing based on drive constraints. *Int J Mach Tool Manuf* 51(12):958–965
17. Beudaert X, Lavernhe S, Tournier C (2012) Feedrate interpolation with axis jerk constraints on 5-axis NURBS and G1 tool path. *Int J Mach Tool Manuf* 57:73–82
18. Erkorkmaz K, Layegh SE, Lazoglu I, Erdim H (2013) Feedrate optimization for freeform milling considering constraints from the feed drive system and process mechanics. *CIRP Ann Manuf Technol* 62(1):395–398
19. Sun YQ, Giblin DJ, Kazerounian K (2009) Accurate robotic belt grinding of workpieces with complex geometries using relative calibration techniques. *Robot Comput Integr Manuf* 25(1):204–210